Determination of electron beam mean incident energy from d_{50} (ionization) values

Randall K. Ten Haken[a] and Benedick A. Fraass
Department of Radiation Oncology, University of Michigan Medical School, Ann Arbor, Michigan 48109

(Received 13 March 1987; accepted for publication 30 June 1987)

Depth-ionization measurements have been obtained with an air-filled Nordic Association of Clinical Physicists (NACP) design parallel-plate ionization chamber in a water phantom for ten foil-scattered electron beams from two different machines with nominal energies between 6 and 20 MeV and field sizes from 6×6 to 25×25 cm^2. Depths of 50% ionization and practical range have been determined from least-squares fits to both the raw data and values corrected to parallel-beam geometry using measured virtual source distances. Depths of 50% dose have also been obtained from fits to divergence-corrected depth-dose measurements performed under identical conditions using, a *p*-type silicon diode detector. Utilizing accepted conversion factors between mean incident energy ($\overline{E_0}$) and depth of 50% dose for parallel incident beams, and taking advantage of the fact that *p*-type silicon diode detector readings are nearly directly indicative of relative dose, conversion factors between $\overline{E_0}$ and depth of 50% ionization for divergence-corrected and raw, uncorrected finite source–surface distance depth-ionization data are empirically determined. Those values, obtained using the results of both ETRAN and EGS4 dose calculations as base lines, are compared to values currently recommended for use in clinical dosimetry.

I. INTRODUCTION

The recent AAPM protocol for calibration of electron beams (TG-21) has made many recommendations to standardize electron dosimetry in the United States.[1] Similar protocols have been adopted by other national and international bodies.[2–4] A basic component of each is the adoption of water as the dosimetry medium of choice. For determination of dose-to-water from air ionization chamber measurements, one needs to correct the ionization reading at each depth by the proper ratio of water and air restricted stopping powers. Those water/air stopping-power ratio values decrease significantly with the average energy of the electron fluence; thus, care must be exercised in their use. In the TG-21 protocol, the stopping-power ratio used to correct an individual measurement is obtained from values presented in tables generated by Berger for plane-parallel, infinitely wide beams of monoenergetic electrons.[1,5] The mean energy at the phantom surface ($\overline{E_0}$) and the depth of the effective point of measurement (Z) are used as input data for interpolation among the table values. Here, ($\overline{E_0}$) is generally determined from analysis of measured depth-dose or depth-ionization data.

An average constant of proportionality (2.33 MeV/cm) between $\overline{E_0}$ and the depth of 50% relative dose, d_{50}(dose) has been noted from analyses of depth-dose curves computed by Berger and Seltzer using forms of the Monte Carlo code ETRAN[6] for plane-parallel, infinitely wide beams of monoenergetic electrons incident upon a semi-infinite water phantom.[1,7] That average conversion factor value is in agreement with the results of an earlier assessment of depth-dose curves of broad beams from medical accelerators by Brahme and Svensson.[4,8] More recently, Rogers and Bielajew have made similar calculations using a different electron–photon Monte Carlo code EGS4[9] and compared them to experimental data.[10] The results of those calculations yield conversion factors between $\overline{E_0}$ and d_{50} (dose) for parallel incidence electron beams that differ from the ETRAN results.

However, the method of $\overline{E_0}$ determination recommended by TG-21,[1,11] is to apply the value 2.33 MeV/cm to the depth of 50% reading obtained from raw ionization (not dose) data, without correction to parallel-beam geometry. The clear deviation of that procedure from use of divergence-corrected dose data was discussed by Wu *et al.*[12] They computed ratios of $\overline{E_0}$ to d_{50}(ion) expected for divergence-corrected depth-ionization curves using Berger and Seltzer's data. Those values range from 2.46 to 2.29 for electrons with mean incident energies between 6 and 50 MeV. They propose the use of their median value (2.38 ± 0.08 MeV/cm) for use with divergence-corrected ionization data. For determinations from raw ionization data, where the divergence dependence also has not been removed, one expects yet another average value (if appropriate) to apply.

We have attempted here to measure the relationships among the depths of 50% reading for divergence-corrected ionization data, raw uncorrected ionization data, and divergence-corrected dose data; all for purposes of mean incident energy determination. Direct determination of the $\overline{E_0}$ would require knowledge of the complete electron energy spectrum at the phantom surface. This is obviously quite difficult to do in a clinical setting and was not attempted. Instead, $\overline{E_0}/d_{50}$ conversion factors appropriate for use with ionization data were indirectly determined assuming: (a) that conversion factors between divergence-corrected dose data and mean incident energy are known, and (b) that relative measurements made with a *p*-type silicon diode detector may be interpreted nearly directly as readings of relative dose. Thus, for a given $\overline{E_0}$, the ratio between the depth of 50% reading for a given divergence-corrected depth-ioniza-

 0094-2405/87/060985-07$01.20

tion curve, $d_{50}(\text{ion})$, and the corresponding value from a divergence-corrected depth-dose curve, $d_{50}(\text{dose})$, will be inversely proportional to the ratio of the conversion factors (CF's):

$$(\text{new CF}) = \frac{\text{known dose CF}}{d_{50}(\text{ion})/d_{50}(\text{dose})} . \quad (1)$$

The relationship in Eq. (1) also applies to determination of a conversion factor, $\overline{E_0}/d'_{50}(\text{ion})$, for uncorrected ionization data, where, as throughout the paper, primed (') symbols refer to quantities not corrected for beam divergence.

We have also investigated how the depth defined as being representative of the practical range,[4] R_p, changes with data type. All measurements will be described in detail, along with a presentation of the data reduction required to quantitatively define the specific depth parameters. Analysis and discussion will follow.

II. MATERIALS AND METHODS

Measurements were made at SSD = 100 cm for the single-foil scattered and dual-foil scattered electron beams generated by Varian Clinac 18 and Clinac 1800 linear accelerators, respectively.[13] Data were obtained using square field sizes of 6×6, 10×10, 15×15, 20×20, and 25×25 cm^2 for energies of 6, 9, 12, 15, and 18 MeV on the Clinac 18 and energies of 6, 9, 12, 16, and 20 MeV on the Clinac 1800. Although the field sizes and some nominal energies are the same on both machines, the beams themselves are considered to be different due to the use of different scattering systems and transmission monitor chambers. Most of the relationships referenced to in Sec. I, are strictly valid for field sizes of diameter greater than a beam's practical range. Thus, our measurements were limited to those situations.

Ionization chamber and diode detector data were obtained in a Therados RFA3-50 water phantom using the RFA-3 positioner.[14] Its control unit has a stated resolution of 0.1 mm in position and 0.1% in normalized reading. At least 15 cm of water was always presented behind each detector to ensure that the electron beams were fully stopped in the water. Measurements were always performed in the same manner, with detectors moved from deeper to shallower depths along the beam central axis, in order to eliminate backlash. The positioner was routinely checked for linearity and reproducibility of position by comparison to a precision steel ruler. These precautions result in better than 0.2-mm precision for reproducibly positioning the chamber. Temperature and pressure were monitored throughout the course of measurements, and normalization runs at nominal depths of maximum dose were obtained at periodic intervals, to insure the consistency of the data. Bias polarity effects and ion collection efficiencies were checked for each detector. Corrections applied to the raw readings were found to be either very small or negligible for the detectors, biases, and dose rates employed.

The ionization chamber measurements were obtained using a Nordic Association of Clinical Physicists (NACP) design parallel-plate chamber.[14] The chamber, as described by Mattsson *et al.*[15] was designed specifically for electron beam measurements. It is a well-guarded chamber featuring a 0.5-mm graphite front wall and a 2-mm air gap. Perturbation effects are minimized and it exhibits a negligible polarity effect. For measurements in the water phantom, it was encased in a Lucite holder with a thin (0.1 mm) Mylar entrance window. Thus, use of this small volume parallel-plate chamber in a water phantom for central axis relative ionization measurements minimizes the need for corrections to the raw readings, provides a well understood and reproducible geometry, and follows the spirit of protocols such as TG-21 as closely as possible. The complete detector assembly was attached to the scanning arm of the RFA-3 positioner, and it was irradiated perpendicular to its flat surface. For each depth-ionization measurement, the chamber's effective measurement point (center of proximal surface of air cavity, 0.6 mm from front surface of Mylar) was placed at a depth approximately $3\times$ the estimated practical range, and measurements were obtained at decreasing depths to within a few millimeters of the water surface. A second, small-volume-thimble ionization chamber was positioned at the periphery of the radiation field and used as a monitor chamber for each set of measurements. Both chambers were placed at a bias of 300 V and ionization measurements were obtained using the standard RFA-3 preamplifier–electrometer system.

Measurements were also obtained for the same energies and field sizes using a p-type silicon diode field detector in the short circuit mode.[14] It is a p–n junction detector made on p-type silicon (which overcomes nonlinearity problems due to radiation damage-induced traps associated with previous n-type silicon diodes).[16–18] It has an effective detector volume of approximately 0.5 mm^3 and an effective thickness of about 0.05 mm in the beam direction. The diode itself is encapsulated in an epoxy cylinder such that the sensitive volume is located less than 0.5 mm below the front face of the detector assembly. The epoxy cylinder is in turn attached to a thin shaft which was attached to the same RFA-3 positioner used for the ionization chamber measurements. A second, reference detector assembly consisting of four diode detector elements connected in parallel was situated at the corner of the radiation field and used as a monitor detector, in a fashion similar to the ionization chamber measurements described above. Readings were obtained as a function of depth in the water phantom using the same RFA-3 electrometer as above.

All relative ionization versus depth data were obtained under the control of a microcomputer.[19] A field detector was moved from its starting position, stopped, and held fixed at each data point, where readings of field current normalized to the monitor detector current were averaged until they showed a variance of less than 0.2%. The detector was then slowly and automatically scanned until reaching either (1) a location 1 cm shallower in depth, or (2) a point receiving a test relative current reading with a 0.5% change from the previous data point, whichever occurred first. At that location, readings were again averaged and defined as another data point. This automatic system of obtaining data insures both accurate and reproducible positioning of the chambers, as well as fairly precise, noise-free measurements of relative current. Also, the data are automatically stored in digital fashion for subsequent analysis, eliminating uncertainties in-

troduced into normal scanning processes where ink pen plots of relative current versus depth are traditionally obtained for a continuously moving field detector.

III. DATA REDUCTION

Data files containing readings of relative ionization $I'(Z)$ vs depth (Z) were used as input for an interactive computer program written specifically for analysis of electron depth-dose/ionization data in the spirit of recent dosimetry protocols.[1-4] Separate data files of divergence-corrected ionization were also generated by applying corrections to the raw data,

$$I(Z) = I'(Z)[(\mathrm{VSD} + Z)/\mathrm{VSD}]^2, \quad (2)$$

using measured virtual-source distances, VSD's.[4] The VSD's were independently measured for each cone and energy by backprojection of the 50% beam widths measured at various distances in air with a small p-type silicon diode. This method yields consistent results with a fairly constant virtual point source position, as are appropriate for the strictly geometric corrections desired here.[20,21]

Comparison of representative samples of the original relative ionization versus depth data for the NACP parallel-plate ionization chamber, the same data corrected for divergence to infinite SSD, and the divergence-corrected diode detector dose data (Fig. 1) reveal slight, noticeable differences among the data types. To facilitate a more quantitative analysis, linear least-squares fits of straight lines were made to the data in the 60% to 30% falloff region and to the bremsstrahlung tail of each curve (Fig. 2). To estimate random uncertainties in the measured quantities due to stopping the detectors for readings, electron beam fluctuations,

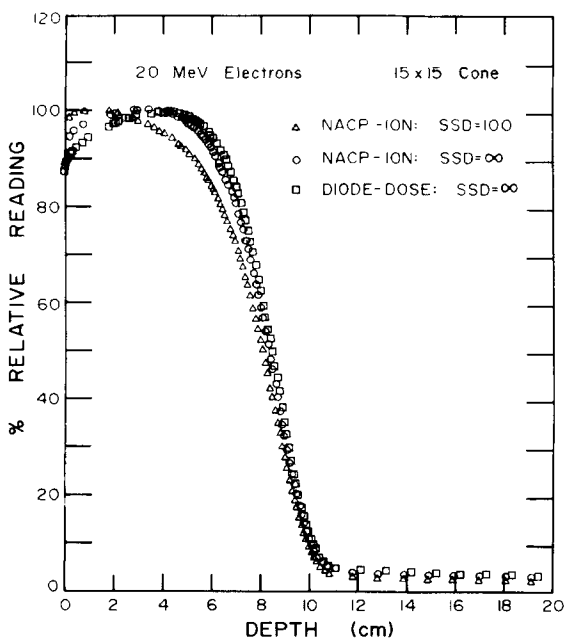

FIG. 1. Representative raw, uncorrected (triangles) and divergence-corrected (circles) NACP chamber depth-ionization data compared to divergence-corrected diode detector depth-dose data (squares). 15×15 cone at 100-cm SSD; 20-MeV nominal incident energy.

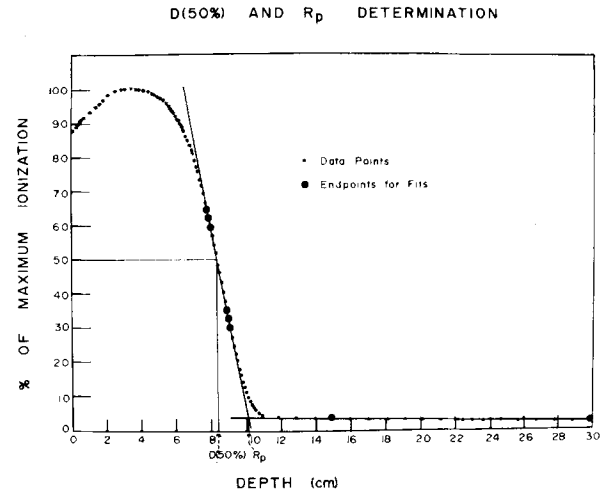

FIG. 2. Sample divergence-corrected percentage depth-ionization data (•) for nominal 20-MeV electron beam in water. Here, ● indicates endpoints used for straight-line fits to data in the falloff region. Depth of 50% ionization calculated from average slope and intercept of the nine possible fits to those two sets of three endpoints each. Also indicated is straight-line fit to data in the bremsstrahlung region. Depth at which that line intercepts average line from falloff region is the practical range.

small changes in detector response, and the statistics of charge collection, data points immediately on either side of original 60% and 30% end points were also identified and used as end points for subsequent fits. Thus, an average slope and an average intercept, along with corresponding statistical standard errors, were determined for each curve. Depths of 50% reading and their statistical errors were computed using the average fit parameters. The bremsstrahlung tails were approximated by fits to all points more than 3 cm beyond the estimated practical range (Enom/2). The depth where that line intersected the average line above was defined as the practical range.[4]

IV. ANALYSIS

The intent here is a determination of multiplicative factors by which the depth of 50% ionization obtained with an air-filled ionization chamber may be related to the mean energy of the electron beam incident on a water phantom ($\overline{E_0}$) such that mass stopping-power ratio data computed assuming a parallel beam of electrons incident on a phantom may be more correctly implemented. We assume that correct individual or average conversion factors between the depths of 50% dose and $\overline{E_0}$ are known for those same conditions of parallel incidence.

The mass collision stopping-power ratios between water and silicon vary much more slowly with energy than the corresponding water/air ratios.[4,5,22] Thus, relative readings obtained with the p-type silicon diode detector are expected to correspond more directly, without need for correction, to measurements of relative absorbed dose in water than would corresponding air ionization chamber measurements. This has been investigated in great detail for electron beams of nominal energy greater than 6 MeV by Rikner and Grusell.[22,23] We have performed similar measurements that agree with their findings.[24] However, for completeness, we

TABLE I. Comparison of divergence-corrected (infinite SSD) air-ionization chamber ionization data and divergence-corrected (infinite SSD) diode detector dose data to $\overline{E_0}/d_{50}$(dose) conversion factors from ETRAN and EGS4 (S.E. = standard error).

(1) *E*-nom (MeV)/machine	(2) d_{50}(dose)(cm) SSD infinity data average	(3) d_{50}(ion)/d_{50}(dose) Data average (± S.E.)	(4) $\overline{E_0}/d_{50}$(dose) SSD infinity ETRAN calc[a]	(5) $\overline{E_0}/d_{50}$(ion) Derived from (4)/(3)	(6) $\overline{E_0}/d_{50}$(dose) SSD infinity EGS4 calc[a]	(7) $\overline{E_0}/d_{50}$(ion) Derived from (6)/(3)
6/CL18	2.26(0.01)	1.002(0.014)	2.43	2.425(0.035)	2.54	2.535(0.035)
6/1800	2.34(0.01)	0.989(0.015)	2.425	2.45 (0.035)	2.53	2.56 (0.04)
9/CL18	3.49(0.01)	0.989(0.008)	2.355	2.38 (0.02)	2.445	2.475(0.02)
9/1800	3.57(0.01)	0.987(0.006)	2.355	2.385(0.015)	2.44	2.47 (0.015)
12/CL18	4.81(0.02)	0.991(0.004)	2.315	2.335(0.015)	2.405	2.425(0.015)
12/1800	4.98(0.01)	0.988(0.007)	2.31	2.34 (0.015)	2.40	2.43 (0.015)
15/CL18	6.09(0.01)	0.987(0.004)	2.29	2.325(0.01)	2.375	2.41 (0.01)
16/1800	6.69(0.02)	0.985(0.004)	2.29	2.325(0.01)	2.37	2.405(0.01)
18/CL18	7.59(0.01)	0.985(0.004)	2.285	2.32 (0.01)	2.37	2.405(0.01)
20/1800	8.53(0.01)	0.983(0.004)	2.28	2.32 (0.01)	2.37	2.41 (0.01)

[a] Obtained from plots in Ref. 10, rounded to nearest 0.005.

have also made water/silicon stopping-power ratio corrections to all the diode data that follow. For the relative quantities and experimental conditions of interest here, resulting values of depths of 50% relative dose or practical range change by less than 0.1 mm from values obtained from diode data where no stopping-power ratio corrections have been made. Hence, given the assumption stated in the previous paragraph, ratios of d_{50}(ion) obtained with the NACP chamber to d_{50}(dose) from the diode measurements should be related to their corresponding $\overline{E_0}/d_{50}$ conversion factors [Eq. (1)].

Weighted average values of the ratios of depths of 50% reading were taken over various field sizes for each beam, with individual ratios being weighted by the inverse square of their uncertainties in the average (Tables I and II, column 3). As mentioned earlier, only field sizes with average diameters greater than a beam's practical range were examined. The average depths of 50% ionization obtained from the raw, uncorrected ionization data are less than the depths of 50% ionization obtained with the same relative data corrected for beam divergence, which are in turn less than the depths of 50% dose obtained from the divergence-corrected diode-dose data. The ratios show no strong trend with energy or field size for the divergence-corrected ionization data comparison (Table I). A trend toward ratio values of lower magnitude with increase in energy is observed for the uncorrected ionization comparison (Table II). This may simply reflect the larger influence of the divergence correction itself on data from beams of higher energy, with their larger depths of 50% ionization and shallower gradients in the fall-off region.

The currently used $\overline{E_0}/d_{50}$ conversion factors for broad parallel monoenergetic beams in water are summarized as a function of depth of 50% dose in a recent paper by Rogers and Bielajew.[10] The values computed using versions of the ETRAN code[6,7] with recent stopping-power ratios[5] and their approximate average of 2.33 MeV/cm form the basis of current practice.[1-4] The more recent EGS4 calculations differ from those results.[10] Here, values of the $\overline{E_0}/d_{50}$(dose) conversion factors for the ETRAN calculations (Tables I and II column 4) were taken from Fig. 13 of Ref. 10 using average depths of 50% dose for the divergence-corrected diode-dose data (Tables I and II column 2). Accepting those ETRAN values as a basis, $\overline{E_0}/d_{50}$(ion) and $\overline{E_0}/d'_{50}$(ion) values were derived [Eq. (1)] for each beam for both divergence-corrected and raw, uncorrected ionization data, re-

TABLE II. Comparison of raw, uncorrected (finite VSD) air-ionization chamber ionization data and divergence-corrected (infinite SSD) diode detector dose data to $\overline{E_0}/d_{50}$(dose) conversion factors from ETRAN and EGS4 (S. E. = standard error).

(1) *E*-nom (MeV)/machine	(2) d_{50}(dose)(cm) SSD infinity data average	(3) d'_{50}(ion)/d_{50}(dose) Data average (± S.E.)	(4) $\overline{E_0}/d_{50}$(dose) SSD infinity ETRAN calc[a]	(5) $\overline{E_0}/d'_{50}$(ion) Derived from (4)/(3)	(6) $\overline{E_0}/d_{50}$(dose) SSD infinity EGS4 calc[a]	(7) $\overline{E_0}/d'_{50}$(ion) Derived from (6)/(3)
6/CL18	2.26(0.01)	0.996(0.014)	2.43	2.44 (0.035)	2.54	2.55 (0.035)
6/1800	2.34(0.01)	0.981(0.013)	2.425	2.47 (0.035)	2.53	2.58 (0.035)
9/CL18	3.49(0.01)	0.982(0.006)	2.355	2.40 (0.015)	2.445	2.49 (0.015)
9/1800	3.57(0.01)	0.979(0.006)	2.355	2.40 (0.015)	2.44	2.49 (0.015)
12/CL18	4.81(0.02)	0.979(0.004)	2.315	2.365(0.015)	2.405	2.455(0.015)
12/1800	4.98(0.01)	0.980(0.006)	2.31	2.36 (0.015)	2.40	2.45 (0.015)
15/CL18	6.09(0.01)	0.968(0.004)	2.29	2.37 (0.01)	2.375	2.455(0.01)
16/1800	6.69(0.02)	0.967(0.004)	2.29	2.365(0.01)	2.37	2.45 (0.01)
18/CL18	7.59(0.01)	0.957(0.004)	2.285	2.385(0.01)	2.37	2.475(0.01)
20/1800	8.53(0.01)	0.956(0.004)	2.28	2.385(0.01)	2.37	2.475(0.01)

[a] Obtained from plots in Ref. 10, rounded to nearest 0.005.

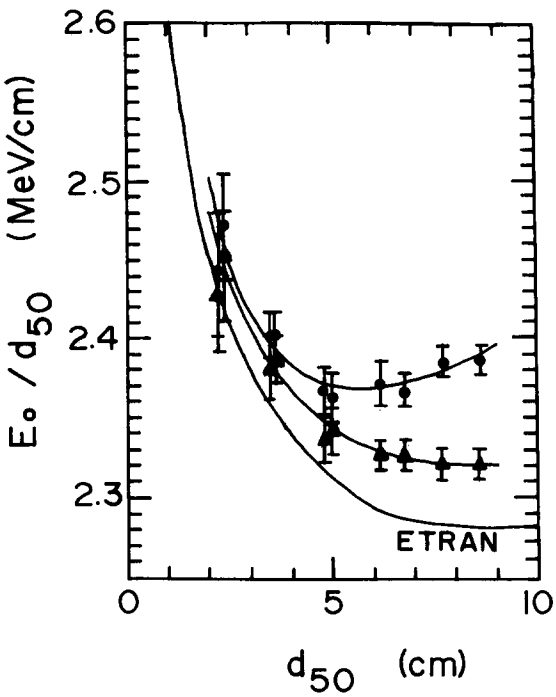

FIG. 3. Comparison of $\overline{E_0}/d_{50}$(reading) conversion factors as a function of d_{50}(reading). ETRAN curve represents $\overline{E_0}/d_{50}$(dose) calculations for monoenergetic, broad, parallel incident beams extracted from Ref. 10. Data points represent $\overline{E_0}/d_{50}$(ion) factors [Eq. (1)] from Tables I and II, respectively, for divergence-corrected (triangles) and raw, uncorrected (circles) air ionization chamber measurements using the ETRAN curve as a base line. Error bars represent standard errors. Smooth curves through data [Eq. (3)] use the least-squares fit coefficients in Table III.

spectively (Tables I and II column 5 and Fig. 3). Also, as per Rogers and Bielajew,[10] fits of the function

$$\overline{E_0}/d_{50} = A + B \ln (d_{50}) + C [\ln(d_{50})]^2, \quad (3)$$

where A, B, and C are coefficients to be determined, were made to the data (smooth curves, Fig. 3) using a least-squares fitting routine with each individual point weighted by the inverse square of its uncertainty in the fit. The computed coefficients (Table III) are only valid for the nominal 6–20 MeV incident energy range studied here. A similar analysis was performed using the EGS4 monoenergetic parallel incidence dose calculations from Fig. 14 of Ref. 10 as a basis (columns 6 and 7, and Table III).

The uncertainties quoted in the average values (Tables I and II) are, as mentioned, standard errors in those average values. As such, they incorporate random uncertainties in the determination of the sample mean values only. One standard deviation in the distribution of individual readings about those means will be larger by an amount approximately equal to the square root of the number of samples used in forming each average (up to five fields). Additional systematic errors on the order of a few tenths of a millimeter may be associated with the initial positioning of the detectors. Those systematic errors, if present, would be constant overall displacements of unknown sign in the depths of 50% reading and practical range. However, their magnitude would be no larger than the statistical uncertainties quoted above. Hence, the uncertainty of values quoted above would at most increase by approximately the square root of two with inclusion of possible systematic sources.

As mentioned earlier, practical ranges were also measured using uncorrected ionization data, divergence-corrected ionization data and dose data. It is expected, and has been pointed out by others,[8,25] that the practical ranges are much less sensitive parameters than are the depths of 50% reading. This was borne out here. Ratios similar to those taken above were obtained for the practical range values and weighted averages over all energies and field sizes again obtained. The ratio of practical ranges determined from the NACP ionization data with divergence correction to the divergence-corrected diode data averaged over all energies and field sizes was 0.998 $\pm$ 0.002 and the ratio of practical ranges determined from the raw uncorrected NACP ionization chamber data to the divergence-corrected diode data was 0.997 $\pm$ 0.003.

TABLE. III. Coefficients for fits of Eq. (3) to $\overline{E_0}/d_{50}$(ion) and $\overline{E_0}/d'_{50}$ (ion) data.

Data		Coefficients		
Table	Column	A	B	C
I	5	2.658	−0.3158	0.07368
II	5	2.723	−0.4126	0.1194
I	7	2.829	−0.4139	0.1013
II	7	2.890	−0.5048	0.1458

V. DISCUSSION

The current status of $\overline{E_0}/d_{50}$(reading) conversion factors is summarized in Fig. 4. The ETRAN curve and the 2.33 MeV/cm AAPM average (solid line) are strictly appropriate for depth-dose curves from monoenergetic beams of plane-parallel incident electrons. The calculations of Wu *et*

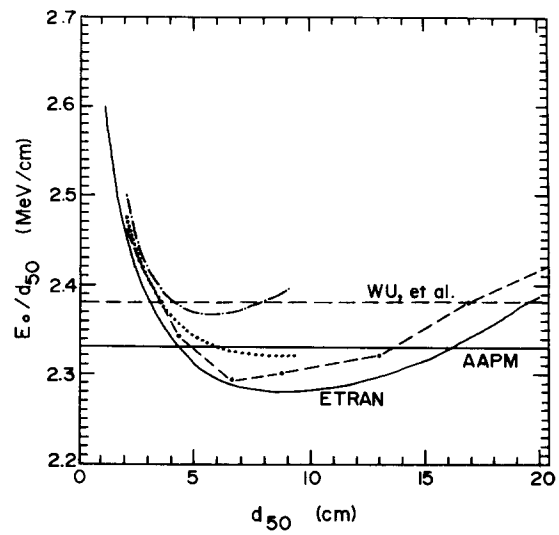

FIG. 4. Comparison of current recommended $\overline{E_0}/d_{50}$(reading) conversion factors relative to the ETRAN base line. ETRAN curve plus AAPM recommended average (solid lines) are from Ref. 10, and are strictly valid for monoenergetic, parallel incident depth-dose curves. Wu *et al.* curve plus average (dashed lines) are computations recommended for corresponding depth-ionization curves.[12] The dotted (divergence corrected) and dot–dashed (finite VSD) curves are fits to the data obtained here for ionization measurements in clinical beams from Fig. 3 via Eq. (1) and Tables I–III.

al. and the average they computed (dashed lines) are proposed for use with depth-ionization curves obtained under similar conditions. The fits of Eq. (3) to the data obtained here (Table III) from measurements of depth-ionization curves in clinical beams, with and without correction to parallel-beam geometry, are represented by the dotted and dot–dash curves, respectively. Deviations from the ETRAN curve are fairly systematic for the divergence-corrected ionization measurements (approximately 1.5% in column 3 of Table I), but increase with increases in beam energy for the raw, finite VSD ionization data (up to 4.5% for 20 MeV). The average values of Eq. (3) (using the parameters in Table III) over the limited energy range studied here are 2.365 and 2.395 MeV/cm, respectively. The divergence-corrected clinical beam ionization results here follow the trend of the Wu *et al.* curve, although they are displaced slightly in magnitude due, perhaps, to the finite energy and angular spread present in clinical beams.

The relationships of the ionization data to the EGS4 base line dose data are qualitatively similar (Fig. 5). That is, Eq. (1) is again used with the same corrections (columns 3, Tables I and II), and only the "known" base line has changed. Displacements of the ionization data from the dose curve are still seen, and they are of the same relative magnitude. However, deviations from the AAPM value have now increased.[10] The SSD = 80 cm values of $\overline{E_0}/d'_{50}$ (dose) computed using EGS4 also differ markedly from the EGS4 dose values for parallel incidence; pointing out the importance of the correction for beam divergence, especially at higher incident energies.[2,10] The shape of the finite VSD dose curve is qualitatively similar to the fit to the raw, uncorrected ionization data here (VSD's approximately 80–90 cm), although displaced in magnitude due to inclusion of stopping-power ratios.

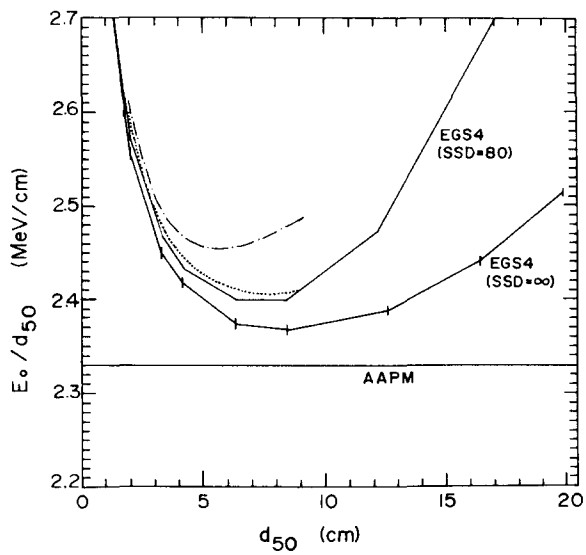

FIG. 5. Comparison of $\overline{E_0}/d_{50}$(reading) conversion factors relative to the EGS4 base line. EGS4 curves (solid lines) are from Ref. 10, and are strictly valid for monoenergetic, parallel incident and SSD = 80-cm depth-dose curves. The dotted (divergence corrected) and dot–dashed (finite VSD) curves are fits to the data obtained here for ionization measurements in clinical beams [Eq. (1) and Tables I–III].

It has been pointed out[4,10,26] that $\overline{E_0}$ may not always be accurately specified by d_{50}(reading) regardless of base line (ETRAN or EGS4), due to differences in the energy spread of incident electron spectra, changes of those spectra with depth, straggling, etc. Also, for clinical beams, the appropriateness of using monoenergetic stopping-power ratios, especially at larger depths, must always be called to question. The measurements performed here were for foil-scattered broad-field clinical electron beams only. Certainly, additional measurements at higher energies, on machines by other manufacturers, and especially on accelerators with scanning beams and narrower energy spreads would provide additional useful information.

We support the contention that, for more precise determinations of mean incident energies from depth-ionization data, values of $\overline{E_0}/d_{50}$(dose) obtained from divergence-corrected dose data do not strictly apply. It is argued[11,27] that the errors introduced through use of the constant 2.33 MeV/cm for even uncorrected ionization data are small. That is, the differences in the values of $\overline{E_0}$ obtained are greater than the differences in values of dose resulting from their use in determining stopping-power ratios. However, as stated by Wu *et al.*,[12] it would seem appropriate that any protocol in use should be as free of "ambiguities and inconsistencies" as possible. We also concur with Rogers and Bielajew that values of $\overline{E_0}/d_{50}$(reading) are appropriately obtained from curves or parameterizations as a function of d_{50}(reading).[10] The results of the measurements presented here provide a basis for the more correct use of depth-ionization data. Clearly, correction of raw ionization data to infinite SSD and use of calculated or empirically determined divergence-corrected ionization relationships will yield more consistent results for all energies.

ACKNOWLEDGMENTS

The authors wish to thank Karen M. Hutchins, M.S. for her careful crafting of the ink drawings and Ms. Michelle McKee and Ms. Karen Gallo for their help in producing the manuscript.

[a] Address correspondence to: Randall K. Ten Haken, Ph.D., University of Michigan Medical Center, Department of Radiation Oncology, AGH-Room B2C490, Box 0010, 1500 E. Medical Center Drive, Ann Arbor, MI 48109.

[1] Task Group 21, Radiation Therapy Committee, AAPM, "A Protocol for the Determination of Absorbed Dose from High-Energy Photon and Electron Beams," Med. Phys. **10**, 741 (1983).

[2] Nordic Association of Clinical Physics, "Procedures in External Radiation Therapy Dosimetry with Electron and Photon Beams with Maximum Energies Between 1 and 50 MeV," Acta Radiol. Oncol. **19**, 55 (1980).

[3] Nordic Association of Clinical Physics, "Electron Beams with Mean Energies at the Phantom Surface Below 15 MeV," Acta Radiol. Oncol. **20**, 401 (1981).

[4] International Commission on Radiation Units and Measurements, Report No. 35, "Radiation Dosimetry: Electron Beams with Energies Between 1 and 50 MeV" (ICRU, Bethesda, MD, 1984).

[5] M. J. Berger and S. M. Seltzer, *Stopping Powers and Ranges of Electrons and Positrons*, 2nd ed., NBS Report No. 82-2550-A (U. S. GPO, Washington, DC, 1982).

[6]M. J. Berger and S. M. Seltzer, "ETRAN, Monte Carlo Code System for Electron and Photon Transport Extended Media," Documentation for RSIC Computer Code Package CCC-107, ORNL, 1973.
[7]M. J. Berger and S. M. Seltzer, "Tables of Energy Deposition Distributions in Water Phantoms Irradiated by Point Monodirectional Electron Beams with Energies from 1 to 60 MeV, and Applications to Broad Beams," Natl. Bur. Stand. (U.S.) Report No. NBSIR-82-2451 1982.
[8]A. Brahme and H. Svensson, "Specification of Electron Beam Quality from the Central-Axis Depth Absorbed-Dose Distribution," Med. Phys. **3**, 95 (1976).
[9]W. R. Nelson, A. Hirayama, and D. W. O. Rogers, "The EGS4 Code System," SLAC Report No. SLAC-265, 1985.
[10]D. W. O. Rogers and A. F. Bielajew, "Differences in Electron Depth-Dose Curves Calculated with EGS and ETRAN and Improved Energy-Range Relationships," Med. Phys. **13**, 687 (1986).
[11]R. J. Schulz, P. R. Almond, G. Kutcher, R. Loevinger, R. Nath, D. W. O. Rogers, N. Suntharalingam, K. A. Wright, and F. M. Khan, "Clarification of the AAPM Task Group 21 Protocol," Med. Phys. **13**, 755 (1986).
[12]A. Wu, A. M. Kalend, R. D. Zwicker, and E. S. Sternick, "Comments on the Method of Energy Determination for Electron Beams in the TG-21 Protocol," Med. Phys. **11**, 871 (1984).
[13]Varian Associates, Inc., Radiation Division, 611 Hansen Way, Palo Alto, CA 94303.
[14]Instrument AB Therados, P. O. Box 15027, S-750 15 Uppsala, Sweden.
[15]L. O. Mattsson, K. A. Johansson, and H. Svensson, "Calibration and Use of Plane-Parallel Ionization Chambers for the Determination of Absorbed Dose in Electron Beams," Acta Radiol. Oncol. **20**, 385 (1981).
[16]G. Rikner and E. Grusell, "Effects of Radiation Damage on *p*-type Silicon Detectors," Phys. Med. Biol. **28**, 1261 (1983).
[17]E. Grusell and G. Rikner, "Radiation Damage Induced Dose Rate Nonlinearity in an *n*-type Silicon Detector," Acta Radiol. Oncol. **23**, 465 (1984).
[18]G. Rikner, "Semiconductor Detector Theory," Med. Phys. **13**, 608 (1986) (Abstract); (private communication).
[19]B. A. Fraass and R. H. Creecy, "Radiotherapy Beam Data: Automatic Acquisition, Analysis, and Comparison to Calculated Dose Distributions," Radiology **153**, 64 (1984) (Abstract).
[20]J. A. Meyer, J. R. Palta, and K. R. Hogstrom, "Demonstration of Relatively New Electron Dosimetry Measurement Techniques on the Mevatron 80," Med. Phys. **11**, 670 (1984).
[21]A. Jamshidi, F. T. Kuchnir, and C. S. Reft, "Determination of the Source Position for the Electron Beams from a Varian Clinac-2500 Accelerator," Med. Phys. **13**, 942 (1986).
[22]G. Rikner, "Characteristics of a *p*-Si Detector in High Energy Electron Fields," Acta Radiol. Oncol. **24**, 71 (1985).
[23]G. Rikner and E. Grusell, "Semiconductor Detector Dosimetry in Small Electron Fields," Med. Phys. **13**, 609 (1986) (Abstract); (private communication).
[24]R. K. Ten Haken, B. A. Fraass, and R. J. Jost, "Practical Methods of Electron Depth-Dose Measurement Compared to Use of the NACP Design Chamber in Water," Med. Phys. 14, 1060 (1987) (this issue).
[25]P. R. Almond, "Electron Beam Energy Determination," Med. Phys. **12**, 534 (1985) (Abstract).
[26]O. Mattsson, "Comparison of Different Protocols for the Dosimetry of High-Energy Photon and Electron Beams," Radiotherapy Oncol. **4**, 313 (1985).
[27]R. J. Schulz and J. A. Meli, "Reply to Comments of Wu *et al.*," Med. Phys. **11**, 872 (1984).